Two crystal structures of the FK506 binding domain of *Plasmodium falciparum* FKBP35 in complex with rapamycin at high resolution.

Alessandra Bianchin[1], Frederic Allemand[2], Angus Bell[3], Anthony J. Chubb[1], Jean-François Guichou[2]

1 Conway Institute of Biomolecular and Biomedical Science, University College Dublin, Dublin, Ireland

2 Centre de Biochimie Structurale, CNRS UMR5048, INSERM U1054, Universités Montpellier 1 et 2

3 Dept. of Microbiology, School of Genetics & Microbiology, Moyne Institute, Trinity College Dublin, Dublin, Ireland

Abstract

Antimalarial chemotherapy continues to be challenging in view of the emergence of drug resistance, especially artemisinin resistance in Southeast Asia. It is critical that we identify novel anti-malarial drugs that inhibit new targets with unexplored mechanisms of action. It has been demonstrated that the immunosuppressive drug rapamycin, currently in clinical use to prevent organ transplant rejection, has anti-malarial effects. The *Plasmodium falciparum* target protein is *Pf*FKBP35, a unique immunophilin FK506 binding protein (FKBP). This protein family binds rapamycin, FK506 and other immunosuppressive and non-immunosuppressive macrolactones.

Here we report two crystallographic structures of rapamycin in complex with the FK506-binding domain of *Pf*FKBP35 at high resolution, in both its oxidised and reduced forms. Comparison to the human FKBP12-rapamycin complex reported earlier, the structures reveal structural differences in the β4-β6 segment that lines the rapamycin binding site. Structural differences between the *Plasmodium* protein and the human hFKBP12 include the replacement of Cys-106 and Ser-109 by His-87 and Ile-90, respectively. Cys-106 which is close (4-5 Å) from atoms of rapamycin, suggests possible routes for the rational design of analogues of rapamycin with specific antiparasitic activity. Comparison of the structures with the *Pf*FKBD-FK506 complex shows that both drugs interact with the same binding site residues. These two new structures highlight the structural differences and the specific interactions that must be kept in consideration for the

rational design of rapamycin analogues with anti-malarial activity that specifically bind to *Pf*FKBP35 without immunosuppressive effect.

Keywords
Plasmodium falciparum; FK506 binding domain; *Pf*FKBP35; Rapamycin; antimalarial drug

1. Introduction

Malaria is still one of the most significant human diseases worldwide, with estimates of 124–283 million cases and 367,000–755,000 deaths in 2014, mostly in sub-Saharan Africa (WHO Malaria report, 2014; White *et al.,* 2014). The disease is caused by infection with intracellular parasites of the apicomplexan protozoon *Plasmodium. Plasmodium falciparum* is the most lethal pathogen among the five species that affect humans and it has developed resistance to several antimalarial drugs (White, 2004). The identification of new chemotherapeutic targets and lead compounds will be an important element of the ongoing campaign to eradicate malaria. It was previously shown that the macrolactone immunosuppressants FK506 and rapamycin (Fig. 1a-b) and several non-immunsuppressive FK506 congeners have antimalarial activity (Bell *et al.,* 1994; Monaghan et al, 2005). The apparent receptor in *P. falciparum* is a 35-kDa FK506-binding protein*, Pf*FKBP35 (Braun *et al*., 2003); Monaghan & Bell, 2005; Kumar *et al.,* 2005). The natural functions of FKBPs have seldom been elucidated but most family members, including *Pf*FKBP35, possess peptidyl-prolyl *cis-trans* isomerase (PPIase) activity (Galat, 2003; Monaghan & Bell, 2005; Kumar *et al*., 2005) and some can act as molecular chaperones (Kuzuhara *et al.,* 2004; Monaghan & Bell, 2005) both of which are relevant to protein folding. Among the physiological roles demonstrated for FKBPs are receptor signalling (Riggs *et al.,* 2003), calcium homeostasis (Jayaraman *et al.,* 1992; Cameron *et al.,* 1995), transcription (Yang *et al,.* 1995), protein

trafficking and stability (Shirane *et al.,* 2003; Jinwal *et al.,* 2010; Ahearn *et al.,* 2011) and neuroprotection (Edlich *et al.* 2006). FKBP ligands are being explored as potential therapies for various diseases. For example rapamycin and its derivatives are under investigation for cancer treatment, tuberculosis, Alzheimer's disease, lupus erythematosus and muscular dystrophy (Blackburn & Walkinshaw, 2011).

Unlike most eukaryotes characterised to date, *Plasmodium* lacks a simple, single FK506-binding domain (FKBD) protein like the major human FKBP, hFKBP12. The FKBD of *Pf*FKBP35 shows 44% amino acid sequence identity to, hFKBP12 but has an additional tetratricopeptide repeat (TPR) domain and putative calmodulin binding motif, making it reminiscent of, if not clearly homologous to, certain other human FKBPs, namely FKBP38, FKBP51 and FKBP52. Human FKBP12 is the major receptor for both FK506 and rapamycin but the mechanisms of action, of the two drugs are markedly different. The hFKBP12–FK506 complex allows the formation of a ternary complex with the phosphoprotein serine/threonine phosphatase calcineurin (CaN; PPP3), inhibiting the phosphatase activity and blocking T-cell activation. By contrast, the complex of FKBP12 and rapamycin interacts with the protein serine/threonine kinase mammalian target of rapamycin (mTOR). This complex inhibits the biochemical pathways required for cell cycle progression during T-cell proliferation and blocks cytokine signal transduction. *Pf*FKBP35, despite its similarity in domain architecture to the non-canonical FKBP38, could be considered to have a canonical FKBD because it interacts with both FK506 and rapamycin and possesses the conserved residues in the active site (Fig. 1c). The PPIase activity of *Pf*FKBP35 is inhibited by FK506 and rapamycin with IC_{50} values of 0.32 µM and 0.48 µM, respectively (Monaghan & Bell, 2005).

Unusually, calcineurin phosphatase activity is inhibited by *Pf*FKBP35 in the absence of FK506, at least under some experimental conditions (Monaghan & Bell, 2005; Kumar *et al.,* 2005), suggesting that the antimalarial activity of FK506 may not be mediated by *Plasmodium* CaN. In the case of

rapamycin, any analogy between the immunosuppressive and antimalarial actions appears to be ruled out by the absence of mTOR in *Plasmodium*. This cumulative evidence points to *Pf*FKBP35 as a possible new antimalarial target acting through an unexplored mechanism of action. Previously, Kotaka *et al.* characterized the X-ray complex structure of FK506 bound to the FKBD of *Pf*FKBP35 (Kotaka *et al.,* 2008) and this structure was used as the basis for design of new antimalarial FKBP ligands (Harikishore *et al.,* 2013). In this work we have elucidated the X-ray structure of rapamycin bound to the FKBD of *Pf*FKBP35 to a high resolution of 1.44 Å and 1.40 Å on two orthorhombic crystal forms, for the oxidised and reduced forms of FKBD respectively, which might provide valuable clues for designing novel non-immunosuppressive agents specific for the *Plasmodium* protein. Drugs based on this model should then retain the antimalarial activity of FK506 and rapamycin, while avoiding its immunosuppressive effect. We compare these structures with the previously reported human FKBP12–rapamycin complex. In spite of a ligand-binding site similar to that of hFKBP12, the *Pf*FKBD structures reveal subtle differences in the β4-β6 region that lines the rapamycin binding pocket. Of note, two of its residues are 4-5 Å from the nearest atom of the ligand, providing opportunities to alter the rapamycin compound to increase its specificity in *Pf*FKBP.

2. Materials and methods

2.1 Protein expression and purification

The expression was performed with the pET29-*Pf*FKBD plasmid (Yoon *et al*., 2007), a kind gift from Prof. H.S. Yoon, Nanyang Technological University, Singapore. This vector was transformed into *Escherichia coli* BL21(DE3) and transformed cells were grown overnight at 25°C in ZYM 5052 auto-induced medium (Studier, 2005) supplemented with kanamycin (50 µg/ml). Cells were harvested by 15 min centrifugation at 6000g at 4°C. The pellet was

resuspended in 25 mM $NaPO_4$ buffer at pH 7.5, 500 mM NaCl and 2 mM 2-mercaptoethanol (buffer A) and stored at -80°C. Cells were lysed by sonication and insoluble proteins and cell debris were sedimented by centrifugation at 40000g at 4°C for 30 min. The supernatant was filtered through 0.45-µm filters and loaded onto affinity columns (His Trap FF 5 ml, GE Lifescience), equilibrated with buffer A. Columns were washed with 20 column volumes of buffer A. Proteins were eluted with 20 column volumes of a linear 0–100% gradient of buffer B (buffer A containing 0.5 M imidazole) at 2 ml/min. The peak fractions were analysed by sodium dodecyl sulphate–polyacrylamide gel electrophoresis (SDS-PAGE). Fractions containing *Pf*FKBD were pooled and dialysed overnight at 4°C against 20 mM Tris HCl pH 8.0, 25 mM NaCl and 1 mM dithiothreitol (DTT) (buffer C). The dialysed protein was then loaded on an anion exchange column (HiTrap Q HP 5 ml, GE lifescience). *Pf*FKBD was eluted with 20 column volumes of a linear gradient (0–100%) between buffer C and buffer D (buffer C containing 1 M NaCl) at 2ml/min. Fractions containing *Pf*FKBD were analysed by SDS-PAGE and pooled. The purified protein was dialysed against a conservation buffer containing 20 mM sodium phosphate buffer pH 6.8, 150 mM NaCl, 1 mM DTT, 1 mM *tris*(2-carboxyethyl)phosphine (TCEP), 0,01% w/v NaN_3 and concentrated to 28 mg/ml with a Vivaspin centrifugal concentrator (Sartorius stedim biotech).

2.2 Crystallization

Crystallization trials of *Pf*FKBD–rapamycin complex were conducted with kits from Hampton Research and Qiagen using sitting-drop vapor diffusion at 18°C. Each trial utilized a Microlab Star from Hamilton and a Nano Cartesian from Genomics Solutions dispensing robot with 200-nl drops (1:1 protein:well solution volume ratio) in 96-well sitting-drop plates. Several hits were found and crystals were obtained by mixing equal volumes of a well

solution consisting of 0.1 M MIB buffer (sodium malonate, imidazole and boric acid, molar ratios 2:3:3) pH 7.0, 25% PEG1500 (w/v %) or 0.1 M MMT buffer (DL-malic acid, MES monohydrate and Tris base, molar ratios 1:2:2) pH 7.0, 25% PEG1500 (w/v %) with the solution of *Pf*FKBP35/rapamycin (1/2 molar ratio). Crystals appeared 12–24 h later at 18°C, reaching 0.1 x 0.05 x 0.05 mm. Crystals were cryoprotected by gently removing most of the mother liquor followed by flash-cooling in liquid nitrogen.

2.3 Data collection, structure determination and refinement

Diffraction data were collected on the ID23-2 and ID-29 beamlines at the European Synchrotron Radiation Facility (ESRF) at 100 K and wavelengths of 0.8726 Å and 0.97625 Å to resolutions of 1.44 Å and 1.40 Å, respectively. Data were processed using *XDS* (Kabsch, 2010) and scaled with *SCALA* (Winn *et al.,* 2011). The space group was determined to be $P2_12_12_1$ using *POINTLESS* (Evans, 2011) for both structures. With one subunit in the asymmetric unit for both structures, the Matthews coefficient (V_M) was calculated to be 2.12 $Å^3Da^{-1}$, with an estimated solvent content of 42% for the first structure and the Matthews coefficient (V_M) was calculated to be 2.45 $Å^3Da^{-1}$, with an estimated solvent content of 50% for the second structure (Kanterdjieff & Rupp, 2003). The structures of *Pf*FKBD–rapamycin were solved by molecular replacement with *MOLREP* (Vagin & Teplyakov, 2010) using the *Pf*FKBD–FK506 complex (PDB entry 2VN1, Kotaka *et al.,* 2008) as a search model (ligand and water molecules were removed). The structures were refined using *REFMAC5* (Murshudov *et al.*, 2011) and model building were performed in Coot (Debreczeni & Emsley, 2012). All structural figures were produced using *PyMOL* ("http://www.pymol.org/"). Atomic coordinates and structures have been deposited in the Protein Data Bank with accession codes 4QT2 and 4QT3. Crystallographic data are summarized in Table 1.

3. Results

3.1 *Pf*FKBD–rapamycin complex preparation, crystallization and structure solution

We expressed *Pf*FKBD with a C-terminal His_6 tag for easy purification purposes. Expression and subsequent purification produced highly pure protein with a typical yield of about 140 mg per liter of culture. The specific activity of the recombinant enzyme was measured by monitoring the *cis-trans* isomerization of ALPF peptide (PPIase activity (Kofron *et al., 1991*)). We observed some crystallization hits (~15) using the PACT kit from Qiagen. Two conditions (0.1M MIB pH 7.0, 25% PEG1500 (w/v %) and 0.1M MMT pH 7.0, 25% PEG1500 (w/v %)) gave some crystals with approximate dimensions of 100 X 50 X 50 µm. Two sets of data from these two crystals were obtained at 1.44 Å and 1.40 Å resolution, for 4QT2 and 4QT3 respectively. These crystals belonged in the primitive orthorhombic space group $P2_12_12_1$ with unit cell parameters a = 35.8, b = 48.7, c = 58.9 and a = 49.5, b = 50.2, c = 57.8, for 4QT2 and 4QT3 respectively. Data-collection statistics are summarized in Table 1. The structures were solved by molecular replacement and one copy of *Pf*FKBD was found in the asymmetric unit for both structures. The final models consisted of 122 amino acids (residues 7 to 128) and 125 amino acids (residues 5-129), respectively.

3.2 Characteristics and comparison of the two *Pf*FKBD binding site–rapamycin complex structures

The *Pf*FKBD binding site is composed of an amphipathic six-stranded beta-sheet (Fig. 2a-b), which has a right-handed twist and wraps around the helix, forming the hydrophobic pocket (Kang *et al.,* 2008; Kotaka *et al.,* 2008). We show here that the hydrophobic pocket between the alpha-helix and the beta-sheet is the binding region for rapamycin, as is the case for FK506. The refined crystallographic structures contain 122 and 125 amino acids, respectively; due to high mobility in the crystals some amino acids are missing from the N-terminal ends of each structure. Both

structures present a monomeric structure of *Pf*FKBD binding site in complex with rapamycin and a clear density was observed for rapamycin (Fig. 2f-g). The two *Pf*FKBD–rapamycin structures are almost identical and they can be superimposed with an RMSD of 0.23 Å at their C_α positions (Fig. 3a). The ligands present an RMSD of 0.18 Å (Fig. 3b). The ligand surface area is 2252Å^2 and 2253Å^2 respectively in the two structures. In both structures rapamycin forms H-bonds with Asp-56, Ile-75, Gly-72, Glu-73 and Tyr-101 (Fig. 2c-d-e and Table 2), which are generally conserved amino acids. Van der Waals interactions, for a distance less than 4.5 Å, are listed in Table 2. Two major differences are found between the two structures we obtained for *Pf*FKBD35 complexed with rapamycin. Firstly, Cys-106 is covalently bond to a molecule of dithiothreitol (DTT) for PDB entry 4QT3 and it is in the reduced form for PDB entry 4QT2. This DTT covalent form did not affect the binding mode of rapamycin (Fig. 2c-d-e, Fig. 3b and Table 2). Secondly, the loop form by residues Ser-57 to Val-63 submits some conformational change between the two structures (Fig. 3a). This rearrangement is due to the crystal packing by exposing the side chain of residues of this loop differently to the other monomer. The motion of this loop from residues Ser-57 to Val-63 implicate a different packing and explain the difference in the unit cell parameter where the parameter conserve between the two structures is b for 4QT2 and a for 4QT3. This difference slightly influences the binding of rapamycin to *Pf*FKBD35, we observe small movements in the region which link C16 to C24 of rapamycin (Fig. 3b), without affecting the hydrogen bonds and van der Waals interactions between rapamycin and *Pf*FKBD35 (Fig. 2c-d-e and Table 2). This observation is correlated with the fact that this region of rapamycin is not directly implicate in the binding interaction with *Pf*FKBD35.

3.3 Comparison of *Pf*FKBD35 with hFKBP12 in complex with rapamycin

Comparison of the primary sequence of *Pf*FKBD with that of the archetypal human FKBP protein shows that the FKBD is highly conserved (44% identity) (Monaghan & Bell, 2005). Alignment of hFKBP12, *Pf*FKBD and other parasites FKBDs is reported in Figure 1c, in which identical residues are highlighted by *. The contacts established between rapamycin and *Pf*FKBD are listed in Table 2, allowing direct comparison with the human FKBP12 protein (PDB entry 1FKB) (Van Duyne *et al.,* 1991). Rapamycin forms H-bonds with hFKBP12 active site residues Asp-37, Ile-56, Gln-53, Glu-54 and Tyr-82, which orientate the inhibitor correctly and stabilize the formation of the ternary complex; several residues are involved in hydrophobic interactions, among which His-87 is the most interesting, since it is not conserved in the *Plasmodium* protein. Our *Pf*FKBD–rapamycin structures superimposed on *Hs*FKBP12–rapamycin (1FKB pdb entry, chain A. Van Duyne *et al.,* 1991) shows an RMSD of 0.35 Å, and comparing the ligands the RMSD is 0.21 Å (Fig. 3c-d). The ligand surface area in hFKBP12 is 2294 $Å^2$. Major differences are found within the β4-β6 region where His-87 and Ile-90 in human FKBP12 are replaced with Cys-106 and Ser-109, respectively, in *Pf*FKBD. In the human FKBP12 protein, the side chains of these two residues form a complementary surface to the pyranose moiety of rapamycin and thus play an important role in ligand binding. *Pf*FKBP35 residues, in contrast, are not directly in contact with rapamycin since the distance between the Cys-106 sulfhydryl group and the Ser-109 hydroxyl group are 4.2 Å and 4.3 Å, respectively. The short distance of rapamycin from Cys106 can permit the design of rapamycin analogues that could react (via the insertion of an electrophilic group like Br or Cl, or the introduction of a Michael acceptor on carbones 43 and 49, Fig. 4) with the cysteine in order to achieve selectivity between human and *Plasmodium* protein without immunosuppressive effects. The proteins RMSD at their C_α positions are 0.31 Å and 0.36 Å for the FKBD-1 of hFKBP51 and hFKBP52 respectively (4DRIA and 4DRJ pdb entry, März *et al.,* 2013). These comparisons demonstrated that in all complexes the same hydrogen-bond network is present which is in

agreement with the structural conservation of the fold and the strict residue conservation in the active site.

3.4 Comparison with *Pf*FKBD in complex with FK506

FK506 is smaller in size than rapamycin but the ligand interacting part is common between the two, and the Tanimoto score is 0.934. *Pf*FKBD residues interacting with rapamycin are the same residues, highlighted in 2VN1 structure by Kotaka *et al.* in 2008, interacting with FK506 with a hydrogen-bond network with residues Asp-56, Ile-75, Gly-72, Glu-73 and Tyr-101. In this structure residue Cys-106 and Ser-109 are also not directly interacting with FK506 (3.9 Å and 5.4 Å, respective distance from FK506). *Pf*FKBD in complex with rapamycin can be superimposed to *Pf*FKBD–FK506 (PDB entry 2VN1) with an RMSD of 0.23 Å for 4QT2 and 0.19 Å for 4QT3 (Fig. 3c). The PDB entry 4QT2 demonstrates close similarity with PDB entry 2VN1 (Fig. 3c), although a small rearrangement is observed in the loop formed by residues Asp-27 to Asn-32. This conformational change is due to the crystal packing by exposing the side chain of residues of this loop differently to the other monomer. This region is not implicated in the binding of rapamycin or FK506. On the contrary, comparison of PDB entry 4QT3 with PDB entry 2VN1 show a superposition of the loop form by residues Asp-27 to Asn-32. As observed for the comparison of 4QT2 and 4QT3, the main difference between these two structures (4QT3 and 2VN1) is a rearrangement in the loop form by residues Ser-57 to Val-63 (Fig. 3c).

4. Discussion

FKBPs have been studied for many decades due to their interaction with macrolactones causing immunosuppression. The immunosuppressive drugs FK506 and rapamycin are in use since 2005 and 2008, respectively, for immunosuppressive regimens

after organ transplant. In particular, rapamycin (which acts independently of calcineurin) is the specific drug used after kidney transplant. FK506 and rapamycin are known to have antimalarial activity (Bell *et al.,* 1994; Monaghan & Bell, 2005; Bell *et al.,* 2006 and Kumar *et al.,* 2005), but the mechanism of action in *Plasmodium* is still obscure.

We present here the 3D structure of the *Pf*FKBP35 FKBD in complex with rapamycin at high resolution, and are now able to compare it with the interactions between the drug and other FKBDs already reported and the interaction between *Pf*FKBD and FK506. The *Pf*FKBD–FK506 complex (Kotaka *et al.,* 2008) shows the same H-bond interactions as rapamycin, which also interacts with Gly-72. Rapamycin interactions with *Pf*FKBD are mostly observed with residues conserved in hFKBP12: a total of 5 H-bonds and several van der Waals interactions can be discriminated within the active site. Important structural differences in *P. falciparum* and human proteins are found, for example *Pf*FKBD Cys-106 and Ser-109 are replaced with His-87 and Ile-90 in hFKBP12. Particularly, His-87 interacts with FK506 and rapamycin, orienting and stabilizing the complex. For these reasons, Cys-106 can be selected as ideal inhibitor target amino acid in the active site as a covalent inhibitor should be specific to the plasmodial form. The argument for the development of a thiol reactive rapamycin analogue is further supported by the finding that the reduced form that contains a covalently linked DTT molecule (4QT3) is still able to bind rapamycin, with close proximity of the DTT to its pyranose ring (see Fig. 2d and Fig. 4a) . The addition of thiol reactive groups to this region of rapamycin may yield a covalent inhibitor that shows greater specificity to the plasmodial form of FKBP.

In conclusion, the results presented here highlight the necessary components of the rapamycin molecule to bind to the *Pf*FKBP35 active site, and furthermore the structural differences

with human proteins that might lead the design of specific and non-immuno-suppressive *Plasmodium* inhibitors.

This work was supported by Irish Research Council [UCD Bioinformatics and System Biology PhD program], University of Montpellier, CNRS, INSERM and French Infrastructure for Integrated Structural Biology (FRISBI) ANR-10-INSB-05-01. We thanks Dr Labesse and Dr Trapani for helpful discussion on the results.

Figure 1.

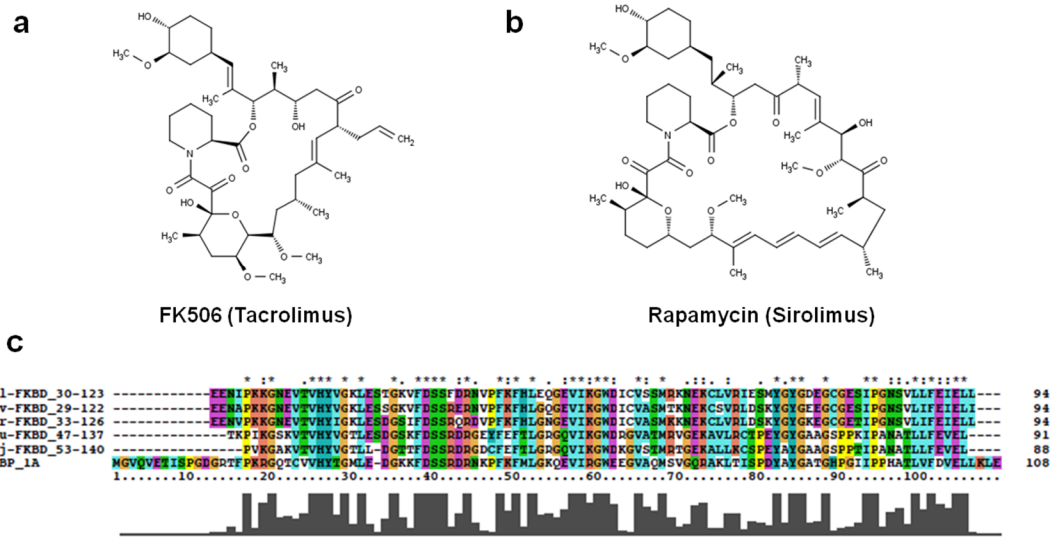

Figure 2.

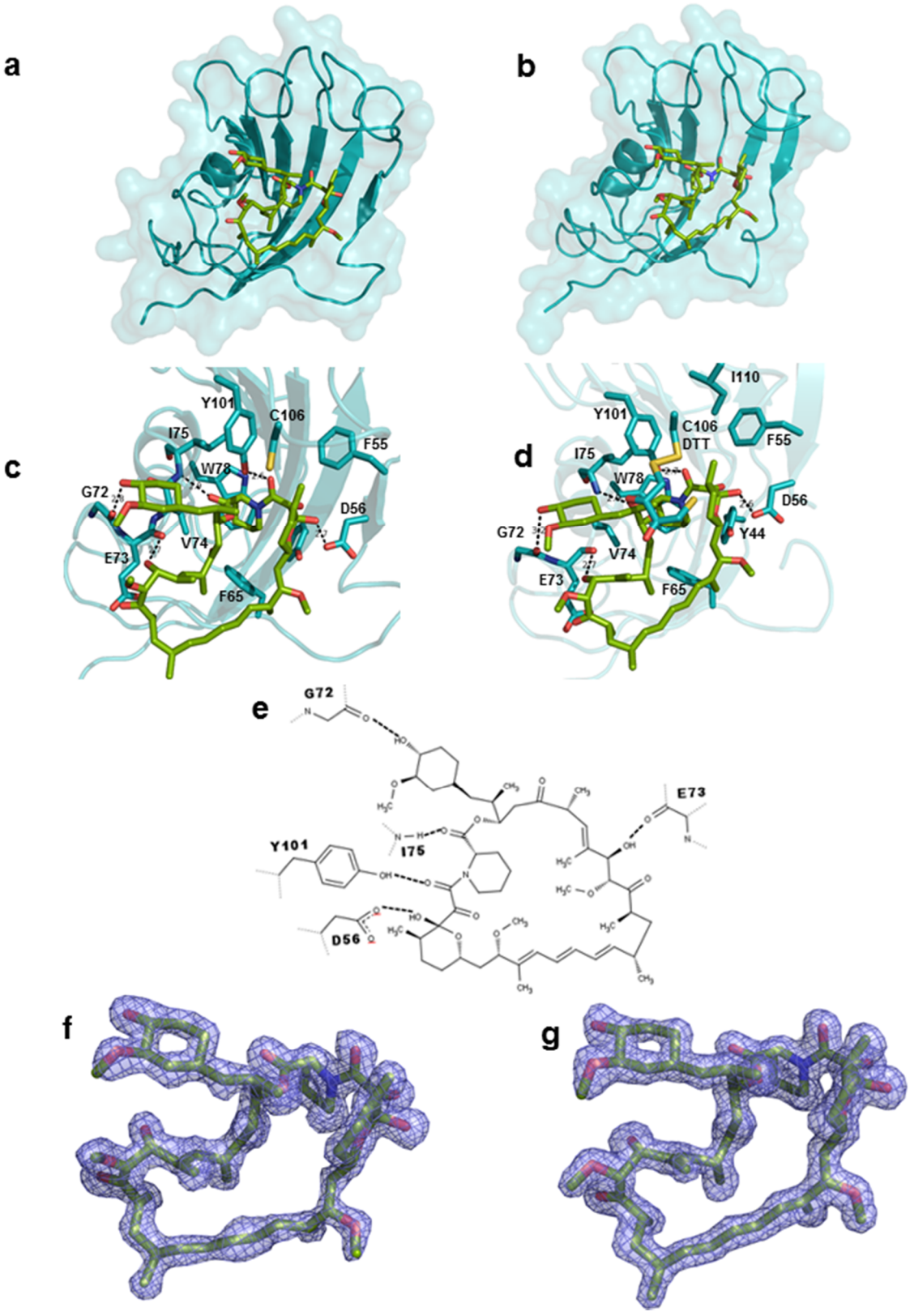
a
b
c
Y101
C106
I75
F55
W78
G72
D56
V74
E73
F65
d
I110
Y101
C106
DTT
F55
I75
W78
D56
G72
Y44
V74
E73
F65
e
G72
E73
Y101
I75
D56
f
g

Figure 3.

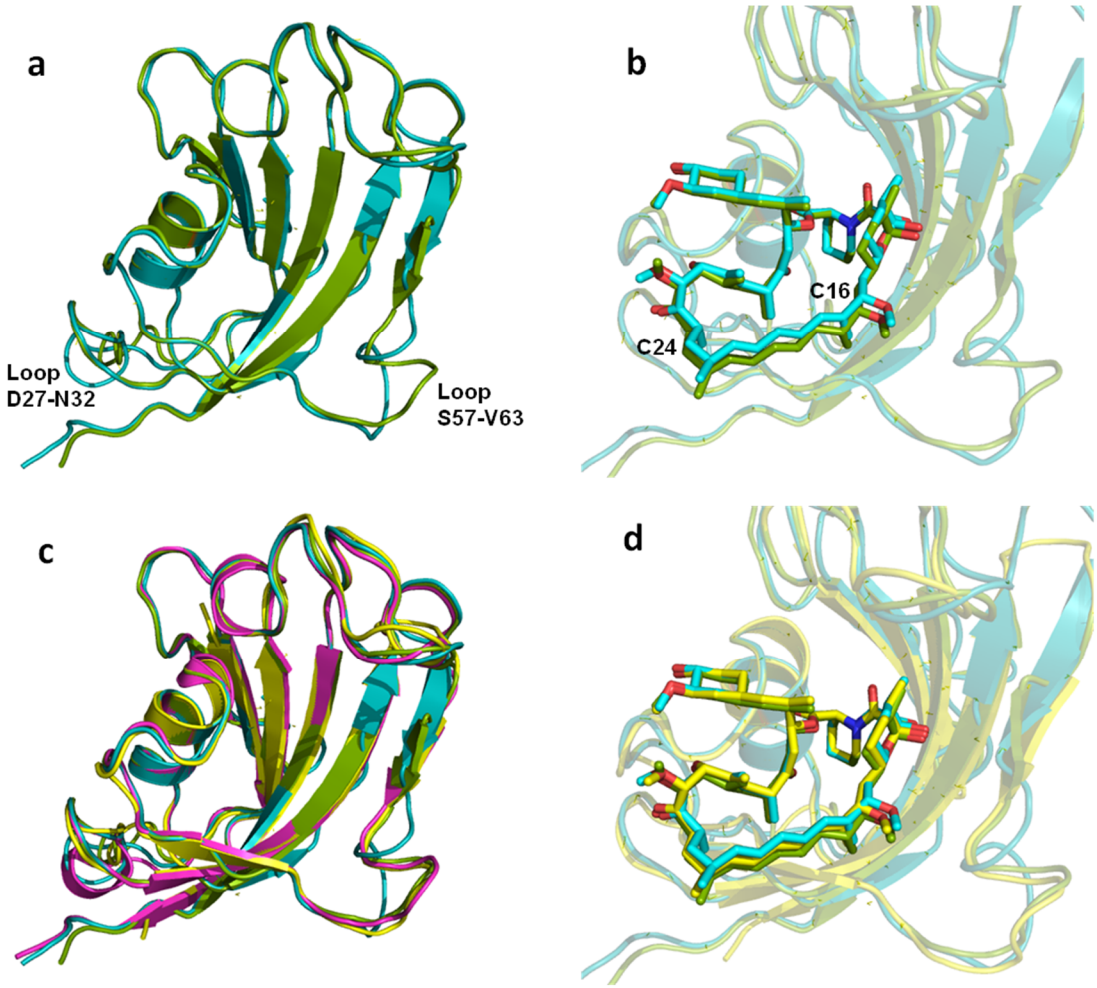

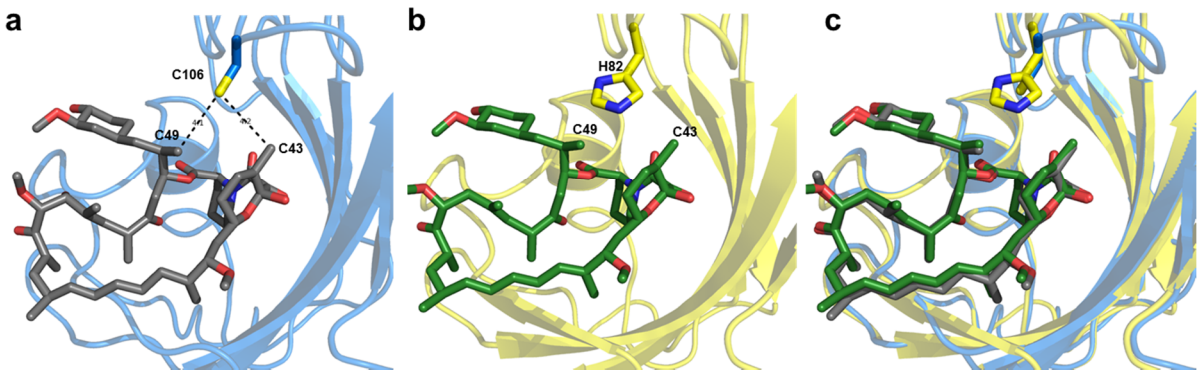

Figure 4.

Tables

Table 1
Data-collection and refinement statistics for *Pf*FKBD-rapamycin complex.

Values in parentheses are for the highest resolution shell.

PDB code	4QT2	4QT3
Data collection		
Space group	$P2_12_12_1$	$P2_12_12_1$
Cell dimensions		
a, *b*, *c* (Å)	35.8, 48.7, 58,9	49.5, 50.2, 57.8
Wavelength (Å)	0.8726	0.97625
Resolution (Å)	30.60 (1.50-1.44)*	50.15 (1.46-1.40)*
Total reflections	75543	124923
Unique reflections	18930	28809
R_{sym} or R_{merge}	0.072 (0.392)	0.032 (0.436)
$I / \sigma I$	6.6 (2.0)	12.0 (1.8)
Completeness (%)	97.8 (89.2)	99.5 (99.4)
Redundancy	3.9 (3.5)	3.7 (3.6)
B-Wilson	12.5	17.9
Refinement		
Resolution (Å)	1.44	1.40
No. reflections	17990	27343
R_{work} / R_{free}	16.20/21.78	14.75/18.71
No. atoms		
Protein	1002	1061
Rapamycin	65	65
Imidazole	5	/
Water	99	152
B-factors (Å^2)		
Protein	16.27	21.79
Rapamycin	14.94	16.73
Imidazole	29.38	/
Water	29.65	34.49
Average B-factors (Å^2)	17.38	23.05
R.m.s. deviations		
Bond lengths (Å)	0.012	0.006
Bond angles (°)	1.813	1.342
Ramachandran plot		
Most favoured regions (%)	98.3	98.3
Allowed regions (%)	1.7	1.7

[AU: Equations defining various *R*-values are standard and hence are no longer defined in the footnotes.]

Table 2
Interactions between rapamycin and *Pf*FKBD

	Nonpolar Contacts*		
ligand region	**4QT2**	**4QT3**	**1FKB**
C2	I-75	I-75	I-56
C3 C4 C5	W-78	W-78	W-59
C4	V-74	V-74	V-55
C5	F-65 V-74	F-65 V-74	Y-26 F-46
C6	Y-44	Y-44	Y-26
C12	**C-106**	**C-106**	**H-87**
C35	Y-101	Y-101	**Y-82**
C42	I-75	I-75	I-56
C43	F-55 **C-106**	F-55 **C-106** I-110	F-36 **H-87 I-90**
C44	F-65	F-49 F-65	F-46
C46	E-73	E-73	E-54
C48	F-65	F-65	F-46
C49	**C-106** Y-101	**C-106** Y-101	Y-82 **H-87**

	Hydrogen Bonds			
ligand	*Pf*FKBD	Donor-acceptor distance (Å) **4QT2** vs **4QT3**	hFKBP	Donor-acceptor distance (Å) **1FKB**
C1 carbonyl	I-75 NH	2.93 - 2.92	I-56 NH	3.02
C8 carbonyl	Y-101 OH	2.61 - 2.66	Y-82 OH	2.76
C10 hydroxyl	D-56 Oβ	2.69 – 2.58	D-37 Oβ	2.74
C28 hydroxyl	E-73 CO	2.75 – 2.74	E-54 CO	2.84
C40 hydroxyl	**G-72 CO**	2.80 – 3.23	**Q-53 CO**	2.75

[*: Non polar contacts are shown for distances < 4.5 Å. In bold the amino acids substitution compared with hFKBP12 (PDB entry 1FKB).]

References

Ahearn, I.M., Tsai, F.D., Court, H., Zhou, M., Jennings, B.C., Ahmed, M., Fehrenbacher, N., Linder, M.E. & Philips, M.R. (2011). *Mol. Cell.* **41**(2):173-185.

Bell, A., Wernli, B. & Franklin R.M. (1994). *Biochem. Pharmacol.* **48**(3):495-503.

Bell, A., Monaghan, P. & Page, A.P. (2006). *Int. J. Parasitol.* **36**(3):261-276.

Blackburn, E.A. & Walkinshaw, M.D. (2011). *Curr. Opin. Pharmacol.* **11**(4):365-71.

Braun, P.D., Barglow, K.T., Lin, Y.M., Akompong, T., Briesewitz, R., Ray, G.T., Haldar, K. & Wandless, T.J. (2003). *J. Am. Chem. Soc.* **125**(25):7575-7580.

Cameron, A.M., Steiner, J.P., Sabatini, D.M., Kaplin, A.I., Walensky, L.D. & Snyder, S.H. (1995). *Proc. Natl. Acad. Sci. USA.* **92**(5):1784-1788.

Debreczeni, J.É. & Emsley, P. (2012). *Acta Cryst.* D**68**(4):425-430.

Edlich, F., Weiwad, M., Wildemann, D., Jarczowski, F., Kilka, S., Moutty, M.C., Jahreis, G., Lücke, C., Schmidt, W., Striggow, F. & Fischer, G. (2006). *J. Biol. Chem.* **281**(21):14961-14970.

Evans, P.R. (2011). *Acta Cryst.* D**67**(4):282-292.

Galat, A. (2003). *Curr. Top Med. Chem.* **3**(12):1315-1347.

Harikishore A., Leow ML., Niang M., Rajan S., Pasunooti KK., Preiser PR., Liu X., Yoon HS. (2013). *ACS Med Chem Lett.* **4**(11):1097-1101.

Jayaraman, T., Brillantes, A.M., Timerman, A.P., Fleischer, S., Erdjument-Bromage, H., Tempst, P. & Marks, A.R. (1992). *J. Biol. Chem.* **267**(14):9474-9477.

Jinwal, U.K., Koren, J. 3rd, Borysov, S.I., Schmid, A.B., Abisambra, J.F., Blair, L.J., Johnson, A.G., Jones, J.R., Shults, C.L., O'Leary, J.C. 3rd, Jin, Y., Buchner, J., Cox, M.B. & Dickey, C.A. (2010). *J. Neurosci.* **30**(2):591-599.

Kabsch, W. (2010). *Acta Cryst.* D**66**(2):125-132.

Kang, C.B., Ye, H., Yoon, H.R. & Yoon, H.S. (2008). *Proteins.* **70**(1):300-302.

Kantardjieff, K.A. & Rupp, B. (2003). *Protein Sci.* **12**(9):1865-1871.

Kofron, J.L., Kuzmic, P., Kishore, V., Colón-Bonilla, E. & Rich, D.H. (1991). *Biochemistry.* **30**(25):6127-6134.

Kotaka, M., Ye, H., Alag, R., Hu, G., Bozdech, Z., Preiser, P.R., Yoon, H.S. & Lescar, J. (2008). *Biochemistry.* **47**(22):5951-5961.

Kumar, R., Adams, B., Musiyenko, A., Shulyayeva, O. & Barik, S. (2005). *Mol. Biochem. Parasitol.* **141**(2):163-173.

Kuzuhara, T. & Horikoshi, M. (2004). *Nat. Struct. Mol. Biol.* **11**(3):275-283.

Larkin M.A., Blackshields G., Brown N.P., Chenna R., McGettigan P.A., McWilliam H., Valentin F., Wallace I.M., Wilm A., Lopez R., Thompson J.D., Gibson T.J. and Higgins D.G. (2007). *Bioinformatics* 23(21):2947-2948.

März, A.M., Fabian, A.K., Kozany, C., Bracher, A. & Hausch, F. (2013). *Mol. Cell. Biol.* **33**(7):1357-1367.

Monaghan, P. & Bell**,** A. (2005). *Mol. Biochem. Parasitol.* **139**(2):185-195.

Monaghan, P., Fardis, M., Revill, W.P. & Bell, A. (2005). *J. Infect. Dis.* **191**(8):1342-1349.

Murshudov, G.N., Skubák, P., Lebedev, A.A., Pannu, N.S., Steiner, R.A., Nicholls, R.A., Winn, M.D., Long, F. & Vagin, A.A. (2011). *Acta Cryst.* **D67**(4):355-367.

Riggs, D.L., Roberts, P.J., Chirillo, S.C., Cheung-Flynn, J., Prapapanich, V., Ratajczak, T., Gaber, R., Picard, D. & Smith, D.F. (2003). *EMBO J.* **22**(5):1158-1167.

Shirane, M. & Nakayama, K.I. (2003). *Nat. Cell. Biol.* **5**(1):28-37.

Studier, F.W. (2005). *Protein Expr. Purif.* **41**(1):207-234.

Vagin, A. & Teplyakov, A. (2010). *Acta Cryst.* D**66**(1):22-25.

Van Duyne, G.D., Standaert, R.F., Schreiber, S.L., Clardy, J. (1991) *J. Am. Chem. Soc.* **113:** 7433.

White, N.J. (2004). *J. Clin. Invest.* **113**(8):1084-1092.

White, N.J., Pukrittayakamee, S., Hien, T.T., Faiz, M.A., Mokuolu, O.A. & Dondorp, A.M. (2014). *Lancet.* **383**(9918):723-735.

WHO (2015). World Malaria report 2014. http://www.who.int/malaria/publications/world_malaria_report_2014/en/

Winn, M.D., Ballard, C.C., Cowtan, K.D., Dodson, E.J., Emsley, P., Evans, P.R., Keegan, R.M., Krissinel, E.B., Leslie, A.G., McCoy, A., McNicholas, S.J., Murshudov, G.N., Pannu, N.S., Potterton, E.A., Powell, H.R., Read, R.J., Vagin, A. & Wilson, K.S. (2011). *Acta Cryst.* **D67**(4):235-242.

Yang, W.M., Inouye, C.J. & Seto, E. (1995). *J. Biol. Chem.* **270**(25):15187-15193.

Yoon, H.R., Kang, C.B., Chia, J., Tang, K. & Yoon, H.S. (2007). *Protein Expr Purif.* **53**(1):179-185.

Figures legends

Figure 1. Chemical structure of immunosuppressant drug and alignment of selected FKBP proteins

(a) Chemical structure of FK506.

(b) Chemical structure of rapamycin.

(c) *Plasmodium falciparum* FK506 binding domain alignment with other FKBD present in different protozoan parasites and with human FKBP12 (made with Clustal X; Larkin *et al.*, 2007).

Plasmodium-falciparum (strain 3D7), NCBI entry XP_001350859.1, FKBDomain amino acids 30-123.
Plasmodium_vivax (strain Sal1), NCBI entry XP_001613999.1, FKBDomain amino acids 29-122.
Plasmodium_berghei (strain ANKA), NCBI entry XP_672280.1, FKBDomain amino acids 33-126.
Trypanosoma_brucei (strain TREU927), NCBI entry XP_828079.1, FKBDomain amino acids 47-137.
Leishmania major (strain Friedlin), NCBI entry XP_001682742.1, FKBDomain amino acids 53-140.
FKB1A_HUMAN protein, UniProt code P62942, full length.

Figure 2. Structure of *Pf*FKBD–rapamycin complex

(a) Cartoon and surface representation of the *Pf*FKBD and stick view of rapamycin (PDB entry 4QT2).
(b) Cartoon and surface representation of the *Pf*FKBD and stick view of rapamycin (PDB entry 4QT3).
(c) Zoom in the binding pocket of rapamycin into *Pf*FKBD showing the binding residues in stick and the hydrogen bonds with lines (PDB entry 4QT2).
(d) Zoom in the binding pocket of rapamycin into *Pf*FKBD showing the binding residues in stick and the hydrogen bonds with lines (PDB entry 4QT3).
(e) Schematic representation of hydrogen network of rapamycin and *Pf*FKBD (PDB entry 4QT2 and 4QT3).
(f) View of the σ_A-weighted 2*Fobs – Fcalc* electron-density omit map of rapamycin contoured at the 1.0σ level (blue) (PDB entry 4QT2).
(g) View of the σ_A-weighted 2*Fobs – Fcalc* electron-density omit map of rapamycin contoured at the 1.0σ level (blue) (PDB entry 4QT3).

Figure 3. Structural comparison of *Pf*FKBD and hFKBP12.

(a) Superposition of the crystal structures of the *Pf*FKBD–rapamycin complexes (PDB entries 4QT2 (green) and 4QT3 (cyan)) showing only the protein as cartoon representation.
(b) Zoom on the rapamycin of the crystal structures of the *Pf*FKBD–rapamycin complexes (PDB entries 4QT2 (green) and 4QT3 (cyan)).
(c) Superposition of the crystal structures of the FKBD–rapamycin complexes (PDB entries 4QT2 (green), 4QT3 (cyan) and 1FKB (yellow)) and *Pf*FKBD–FK506 (PDB entry 2VN1 (pink)) showing only protein as cartoon representation.
(d) Zoom on the rapamycin of the crystal structures of the FKBD–rapamycin complexes (PDB entries 4QT2 (green), 4QT3 (cyan) and 1FKB (yellow)).

Figure 4. Structural comparison of *Pf*FKBD and hFKBP12 for the design of specific inhibitors.

(a) Cartoon representation of the *Pf*FKBD and stick view of rapamycin and residue C-106 (PDB entry 4QT2).
(b) Cartoon representation of the *Pf*FKBD and stick view of rapamycin and residue HIS-87(PDB entry 1FKB).
(c) Supperposition of panel a and b (PDB entry 4QT2 and 1FKB).